

Original Article	Adipose tissue-derived stem cells versus bone marrow-derived stem cells as an angiogenic therapy after ischemic limb injury in the adult male albino rat <i>Mohamed El-Badry Mohamed¹, Mona H. Mohamed Ali², Maha Mohamed Abo-gazia³, Rania Abdel-Azim Galhom² and Amira El-Sayed farage⁴</i> ¹ Department of Human Anatomy and Embryology, Faculty of Medicine, Assiut University ² Department of Human Anatomy and Embryology, Faculty of Medicine, Suez Canal University ³ Department of Histology, Faculty of Medicine, Kafrelsheikh University ⁴ Department of Human Anatomy and Embryology, Faculty of Medicine, Kafrelsheikh University
-------------------------	---

ABSTRACT

Background: Peripheral arterial disease (PAD) remains one of the leading causes of deformity worldwide. Among various therapeutic options for PAD, stem cell-based therapies hold some great promises. Nonetheless, the therapeutic efficacy faces the limitation of poor survival of donor cells.

The aim of this work: Isolation of the rat bone marrow MSCs (BM-MSCs) and adipose tissue MSCs (AD-MSCs) and assessing their growth kinetics and their role in improvement of angiogenesis after induction of acute hind limb ischemia through ligation of the femoral artery of the adult male albino rat.

Material and Methods: The rat bone marrow and the adipose tissue were isolated from 10 male adult albino rats. They cultured and expanded through 6 passages. Acute lower limb ischemia was done by ligation of unilateral left sided femoral artery of an adult male albino rat. Both BM-MSCs and AD-MSCs, were injected immediately following ischemia in the semimembranosus muscle. BM-MSCs and AD-MSCs biological characteristics evaluated for cell therapy (morphology, flow cytometric analysis, colony-forming unit-fibroblast assay, proliferation capacity at passages 2, 4 and 6, population doubling time (PDT) and cell growth curves). Evaluation of muscle regeneration and angiogenesis was assessed through H&E staining of the tissue, Masson Trichrome to assess fibrosis, CD31 immunostaining for new blood vessel formation and electron microscopic examination for the cells ultrastructure.

Results: BM-MSCs and AD-MSCs attached to the culture flask and displayed spindle-shaped morphology, more evident in AD-MSCs. Proliferation rate of AD-MSCs in the analyzed passages was more than BM-MSCs. The increase in the population doubling time (PDT) of both types of MSCs occurs with the increase in the number of passages. Light , electron microscopy and immunohistochemistry showed the better ability of AD-MSCs in improving the ischemic limb through their angiogenic capacity than BM-MSCs.

Conclusion: Rat AD- MSCs have growth kinetic advantages in the proliferative capacity,colony-forming unite fibroblast, population doubling time and angiogenic capacity when transplanted in a rat model of a hind limb ischemia more than that of BM-MSCs

Received: 01 October 2017, **Accepted:** 26 October 2017

Key Words: Adipose tissue stem cells, adult male albino rat, angiogenesis, bone marrow stem cells, Growth kinetics, hind limb ischemia, mesenchymal stem cells.

Corresponding Author: Mohamed El-Badry Mohamed, Department of Human Anatomy and Embryology, Faculty of Medicine, Assiut University, **Tel.:** +20 1283553122, **E-mail:** melbadry_55@hotmail.com

The Egyptian Journal of Anatomy, ISSN: 0013-2446, Vol. 41. No. 1

INTRODUCTION

The peripheral arterial obstructive disease (PAOD) is a chronic disease that affects approximately 3 to 10% of the population (Gresele et al., 2011). It obstructs the peripheral arteries, leading to decreasing the blood flow and development of limb ischemia or critical limb ischemia (CLI) with a high morbidity and mortality rate of about 25% and an amputation rate of 30% (Das et al., 2013).

Limb ischemia results in cool limbs, ischemic rest pain, non-healed ulcers, gangrene, and absent distal peripheral pulses which varies per the degree of obstruction and may increase the risk of the limb loss (Mees et al., 2011 and Hart et al., 2013).

Transplantation of mesenchymal stem cells (MSCs) derived from the bone marrow, placenta or umbilical cord significantly facilitated angiogenesis in animal models of the hind limb ischemia (Liu et al., 2015 & Xie et al., 2016). Genetically modified stem cells encoding (VEGF), (FGFs), hepatocyte growth factor (HGF) were also used as possible therapeutic agents and proved to increase the vascular density and form collaterals in the ischemic skeletal muscle (Katara et al., 2013, Shimamura et al., 2013 and Yin et al., 2015). The regenerative effect of stem cells was explained by their differentiation in the regenerating tissue or by their paracrine regulation of growth and trophic factors (Yin et al., 2016).

Although the bone marrow has been considered as a main source for isolation of multipotent MSCs for clinical use, the related pain, side effects, and morbidity during their harvest in addition to the low cell yield considered to be great limitations (Wang et al., 2012). Unlike the bone marrow, the adipose tissue is a rich source of stem cells that can be collected easily in a sufficient yield with a minimal morbidity, less time and expense required to generate a therapeutic cell dose (Baer & Geiger, 2012).

MSCs proliferation and senescence have been used for cytototherapy. In vitro culture and expansion of MSCs is a must to provide a sufficient yield of a pure cell population for the clinical applications. During this expansion process, cells growth, proliferation, potency and protein expression change (Kretlow et al., 2008

& Jo et al., 2008). Comparative studies of the growth kinetics of BM-MSCs and AD-MSCs are lacking. Therefore, the aim of this study was to isolate, culture and compare the rat BM-MSCs and AD-MSCs for their growth characteristics and proliferation capacity using growth curve analysis, colony-forming unit fibroblast assay (CFU-F) and population doubling time (PDT). Also, to compare their angiogenesis effect in the rat model of the hind limb ischemia.

MATERIAL AND METHODS

Animals and experimental design: A total of seventy adult male albino rats weighing 200-250 grams (24-week-old) were used in this study. They were divided randomly into five groups 10 rats each, in addition to twenty rats used as a source for BM-MSCs and AD-MSCs 10 rats each. All the procedures are in accordance with Animal Guideline Care of Ethical Committee of Suez Canal University (Ethics Code No. 2498). All applicable institutional and national guidelines for the care and the use of laboratory animals were followed. They were housed under standard conditions for a week prior to use. The five groups: I- The control groups, each animal was exposed to an incision of the skin and an exposure of the femoral artery without its ligation, II- The positive control, ischemic group, in which all the animals were exposed to the femoral artery ligation and received DMEM once as an intramuscular injection and sacrificed 6 weeks after. III&IV- The treated groups which include; the ischemic-BM-MSCs treated group and the ischemic-AD-MSCs treated group; their animals were exposed to the femoral artery ligation and received BM-MSCs and AD-MSCs respectively as a single intramuscular injection and sacrificed 6 weeks after.

Isolation and culture of AD-MSCs (Niyaza et al., 2012)

The animals were sacrificed by cervical dislocation. The omental and the pre-renal adipose tissue were isolated and collected in 15-ml sterile tubes. Under sterile conditions, the excised adipose tissue was rinsed with phosphate-buffered saline (PBS), (Sigma-Aldrich), cut into small pieces and digested with collagenase type I (0.1%) (Sigma-Aldrich) at 37°C for 30 minutes. The collagenase effect was blocked with Dulbecco Modified Eagle Medium (DMEM) supplemented

with 10% fetal bovine serum (FBS),(Gibco) and centrifuged at 1800 rpm for 10 minutes. The pellet was then filtered through a 200 µm stainless steel mesh (Sigma) to remove undigested tissue. Adipose digested cells were suspended in a DMEM supplemented with 10% FBS, 1% penicillin and streptomycin (Sigma-Aldrich) and cultured in 75-cm² flasks. The cultures were incubated at 37°C with 5% CO₂ and saturated humidity. The first culture media was changed after 24 h to remove the non-adherent cells and the adherent cells were maintained in the culture. The subsequent medium exchange was performed every 3-5 days till the cultures approximately 80-90% confluence. The adherent cells were washed twice with PBS and the cells were harvested using 0.25% trypsin (Gibco) for 5-10 min and the enzyme was inactivated with the same amount of complete culture media. AD-MSCs were passaged up to 6 times. At each passage the cells were counted microscopically using a hemocytometer and analyzed for the cellular growth.

BM-MSCs isolation and culture (Yoshimatus et al., 2015):

Under sterile condition both femur and tibia from the rats were dissected and carefully shaved of adherent flesh using a sharp sterile blade. The ends of the bones were cut and the bone marrow was harvested in a 15 ml Falcon tube by flushing with 10 ml syringe with DMEM. After washing and centrifugation at 1800 RPM for 10 minutes, cell pellet was collected, re-suspended in a DMEM medium supplemented by 10% FBS with antibiotics and cultured in a 75-cm² flask. The cultures were incubated at 37°C in a 5% CO₂ environment and a saturated humidity. After incubation, the culture media was changed and passaged as described before for AD-MSC.

Characterization of the cultured cells:

Flow cytometry analyses of the cultured cells on a BD FACS Calibur flow cytometer (BD Biosciences), for CD34, CD44 was performed for both AD-MSCs and BM-MSCs at P3 (Terai et al., 2003).

Growth kinetics: growth curves, Colony forming unite fibroblast assay (CFU-F assay) and Population doubling time (DT) of the cultured cells:

Growth curves of BM-MSCs and AD-MSCs were plotted to compare growth kinetics of them (Peng et al., 2008). Cellular Growth rate and expansion during the passaging from P2 to P6 was performed to both types of stem cells. The second passage started with 1.5X10⁵ cells then the cells were counted every passaging till the 6th one. For the assessment of growth characteristics, BM-MSCs and AD-MSCs at passages 2, 4 and 6 were seeded in a 24-multi well plate at a density of approximately 5×10⁴ cells per well plate. Cells were collected from each well 1 to 7 days after seeding and counted to produce cell growth curves. to compare the colonogenic potential of the two types of stem cells, ten tissue culture flasks of both AD-MSCs and BM-MSCs containing 1x10⁶ cells/each, of 1st passage, were cultured for 14 days then fixed with acetone/methanol, volume to volume and stained with Giemsa stain. Cell colonies of more than 50 cells were counted then the mean ± SD was estimated (Kakudo et al, 2014). For doubling time experiments, 20,000 cells from both type of cells were plated in a 75 cm² flask and counted at 48, 72 and 96-hour time points. The population doubling time for each time point was calculated using the formula: $DT = n \times \log_{10} (2n/m) / \log_{10} t$; where, n=number of cells at the beginning of the time period, m=number of cells counted at the end and t =time period. Thus, the doubling time was ascertained from at least 3 time points and the mean was calculated accordingly (Yoshimatsu et al., 2015).

Induction of a rat model of unilateral hind limb ischemia: (Huang et al., 2008 and Xie et al., 2016):

Under complete aseptic conditions and after complete anesthesia with intraperitoneal injection of sodium pentobarbital prior to experiments (40mg/kg) the animal was placed in a supine position onto the pre-operating table. The hair of the left hind limb was shaved carefully and sterilization of the whole limb and lower abdomen took place. A longitudinal incision was made along the left medial thigh. Using a clean set of fine forceps and cotton swab, dissection and separation of the femoral artery from the femoral vein and nerve at the proximal location near the groin was done carefully. The proximal portion of the femoral artery was ligated with silk ligatures and the incision was closed. Then the animal was placed on top of a draped heated pad in the recovery cage to guard against hypothermia

and monitored continuously until awake. Post-operative analgesics and antibiotics were used to relieve the pain and prevent the infection.

Injection and euthanization of the animals:

The stem cells from both sources were trypsinized from p 2-5 and washed. After testing the viability of the cells, using a trepan blue exclusion assay, a dose of 3×10^6 cells /ml was suspended in 0.5 ml of DMEM as a vehicle and injected in the semimembranosus muscle of each rat of the treated groups III&IV, just after the ischemic injury. The ischemic group received 0.5 DMEM only. The rats were euthanized 6 weeks after the induction.

Histopathological assessment:

For each rat, the bilateral semimembranosus muscles were removed and weighed a paraffin block from each muscle was prepared and serial 5 micrometers thick tissue sections were obtained from each block, stained with hematoxylin and eosin (H&E) and Masson trichrome for histopathological assessment. To assess muscle fiber regeneration after ischemia the number of muscle fiber /mm² was calculated in (H&E) sections also fibrotic areas and degree of fibrosis were evaluated in Masson trichrome sections. Number of fibers and Fibrotic areas were calculated by averaging the counts of five separate fields in four distinct areas in each specimen using Image J soft were (NIH, Bethesda, MD, USA).

Immunohistochemical tissue analysis:

For immunohistochemical staining, 3-5 micrometer sections were performed dried, deparaffinized followed by dehydration through graded alcohol. The endogenous peroxidase activity was quenched with 3% hydrogen peroxide for 5 minutes. Subsequently, they were incubated a polyclonal rabbit anti-mouse anti-CD31 primary antibody(1:100, Abcam, Cambridge, UK) overnight at 4°C, followed by Alexa Goat Anti-Rabbit IgG secondary antibody at room temperature (1:200, Invitrogen) for one hour. Capillary density and number of capillaries per muscle fiber, were counted. ImageJ software (NIH, Bethesda, MD, USA) to count the number of CD31 positive capillaries. Six sections from each sample were used for the average positive immunoactivity.

Transmission electron microscopy:

After the desired time of ischemia the muscles were perfused with warm (37°C) 4% paraformaldehyde in 0.1 M phosphate buffersaline (PBS), followed by cold 2% glutaraldehyde solution (2% GA in 0.1 M PBS) for a total of 30 minutes. Approximately 1×1 mm pieces of muscles were cut out and post-fixed in 2% glutaraldehyde (1 hour) followed by 1% osmium-tetroxide (in 0.1 M cacodylate buffer, 1 hour at 4°C). Ultrathin sections were prepared with an ultra-microtome, contrast-stained with uranyl acetate and lead citrate. The stained sections were examined and photographed using a Hitachi H7500 transmission electron microscope (Hitachi Ltd, Tokyo, Japan).

Statistical Analysis:

The data are generally expressed as means ±SD. SPSS software version 12.0 (SPSS, Inc., Chicago, IL, USA) was used for statistical analyses.

Statistical significance among mean values was evaluated using analysis of variance (ANOVA) test and Tukey post-hoc test for testing the statistical significance. Probability values of $P < 0.05$ were considered to indicate statistical significance.

RESULTS:

Morphological assessment:

BM-MSCs and Ad-MSCs were isolated from the rats. At the 3rd day of the culture a population of the attached cells to the substratum of the tissue culture flask were observed while the floating round-shaped cells were discarded with the first media exchange. The number of the attached cells increased gradually with maintaining of the culture until reached confluency around the 9th or 10th day after seeding. The attached cells of both types showed heterogeneous morphology with various shapes; flat, star, sperm, triangular and elongated. The cytoplasmic processes of AD-MSCs were longer than that of BM-MSCs (Fig.1).

After passage 2, both types of cells became relatively homogeneous showing a similar morphology with abundant cytoplasm and had large nuclei with multiple nucleoli. The fibroblast-

like appearance was clearly seen in AD-MSCs while the BM-MSCs tended to be polygonal (Fig. 2). The colony formation was evident on both types of cells from the 7th day of 1ry culture through all passages. The colonies of AD-MSCs showed over growth of the cells on each other while cell to cell growth inhibition was seen in the colonies of BM-MSCs (Fig. 2). Fibroblast-like cells were observed in all passages (Fig. 3).

Phenotypic characterization of MB-MSCs and AD-MSCs:

Flow cytometry analysis during the 3rd passage of BM-MSCs and AD-MSCs showed that both types of cells expanded in FBS-supplemented medium. BM-MSCs exhibited specific MSC marker (CD44) at a higher level than that of Ad-MSCs (80% and 65% respectively), and hematopoietic cell markers (CD34) at a lower level than AD-MSCs (9% and 22% respectively). The homogeneity of the phenotype was observed in both types of cells (Fig. 4).

Cellular growth curve and CFU-F assay:

Both AD-MSCs and BM-MSCs showed an exponential growth from P2 to P6, shown by trend lines in Fig. 5, with a maximum population density of BM-MSCs at the 5th passage followed by a recognizable stability from P5 to P6. The number of the cultured attached AD-MSCs exceeds that of BM-MSCs at all passages. This increase was statistically non-significant in passage 2 ($P < 0.5$) and highly significant through the subsequent passages ($P < 0.05$).

Regarding the tendency of colony formation, both AD-MSCs and BM-MSCs showed tendency to form colonies both in the primary culture and the subcultures. There was a significant difference of AD-MSCs colonogenic potential ($9.5 \pm 3.7\%$) in comparison to that of BM-MSCs ($4.7 \pm 1.6\%$) during the 1st passage, $P < 0.05$ (Fig. 6).

Population doubling time (PDT):

To assess the rate of cellular growth the PDT; (the time by which cell population doubles in number) was calculated. AD-MSCs proliferative capacity is significantly more than that of BM-MSCs as PDT of AD-MSCs during the 2nd, 4th and 6th passages were 52.3 h, 61.2 h and 82.5 h, respectively. Also, PDT was 63.6 h, 69.6 h and

93.5 h at the same passages for BM-MSCs (Fig. 7 and Table1).

Histopathological changes associated with the hind limb ischemia:

Gross changes: edema of the scrotum in the ipsilateral side, atrophic changes as ulcer formation and loss of the subcutaneous fat and distal toe necrosis were obviously seen in almost of all the animals of the ischemic group (eight rats were affected over ten rat in the ischemic group), while these symptoms were absent in the treated groups (Fig. 8). The histological section of the semimembranosus muscle of the control group showed well organization of the muscle fibers. The nuclei are arranged peripherally along the fibers, their number vary from one to two in the same fiber. The muscle fibers are separated from each other by distinctive highly vascular connective tissue spaces. The semimembranosus sections of the ischemic group showed degeneration and scattered areas of hemorrhage between the muscle fibers which lack the normal organization of the control group. Both BM-MSC and AD-MSCs treated groups showed restoration of the normal architecture of skeletal muscle and considerable muscle fiber regeneration (Fig. 9). Interstitial fibrosis was obviously seen in the sections of the ischemic group stained with Masson trichrome. Compared to BM-MSCs- treated group and AD-MSCs- treated group the animal of which exhibited significantly less fibrosis (Fig. 10). Quantification of these data revealed marked significant reduction of the number of muscle fiber / mm² in the ischemic group in comparison to the control group the number of which increased significantly in the treated groups in comparison to the ischemic group with no significant difference between the two treated groups. The fibrotic area percentage significantly increase in the ischemic group and reduced in both treated groups with no significant difference between them (Fig.11,12).

Results of new angiogenesis:

Expression of CD-31; a specific endothelial marker was performed to test new angiogenesis. Expression of this marker was obviously seen in both BM-MSCs and AD-MSCs- treated groups on the other hand the ischemic group showed almost no positively stained cells in comparison to the control (Fig.13). Quantification of these results showed that the capillary density (number of CD-

31positively stained cells/ total muscle fiber area) of semimembranosus section of rat model of hind limb ischemia in the ischemic group decreased significantly in comparison to the control group (1.1%, and 3 %, respectively). While a marked significant increase in capillary density in both BM-MSCs-treated group and AD-MSCs treated group was evident (5.7 % and 7%, respectively) with a significant increase in the AD-MSCs treated group in comparison to the BM-MSCs-treated group (Fig. 14).

Results of transmission electron microscopy:

Semimembranosus muscle of the control group showed normal alignment of the Z lines between the muscle fibers and a peripherally situated nucleus was seen between the muscle fibers. Large numbers of mitochondria with

different size and well-developed cisternae were also seen. Blood vessels were also seen in some sections (Fig.15). The ultrastructural sections of the semimembranosus muscle of the ischemic group showed distortion of the normal alignment of the Z lines and loss of general arrangement of muscle fibers. Some mitochondria with abnormally ruptured cisternae were evident (Fig.16). The ultrastructural sections from the semimembranosus muscle from ischemic groups treated with BM-MSCs and AD-MSCs showed plenty of newly formed blood vessel, reconstruction of the muscle fibers and restoration of their normal architecture specially in the AD-MSCS treated group and scattered numbers of mitochondria were seen in BM-MSCS treated group while large number of them, with well-developed cisternae arranged in line were observed in the AD-MSCs treated group (Fig. 17)

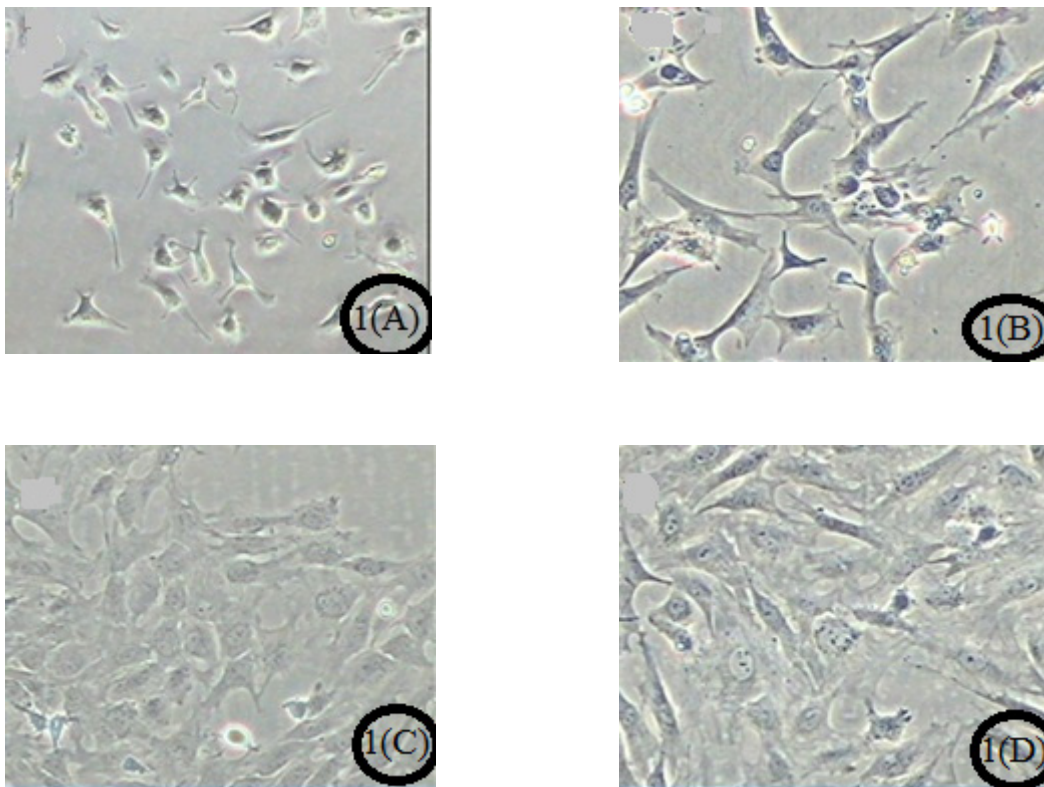


Fig. 1: A phase contrast of rat BM-MSCs {1(A, C)} and AD-MSCs {1 (B&D)} in primary culture 3 days after seeding {1(A&B)} and 10 days after seeding {1(C, D)}. The cells were attached to the substratum and took different morphological appearance. AD-MSCs possess longer cytoplasmic process 1(B) and reached about 95% confluency by the 10th day post seeding {1(D)}. Scale Bar 100

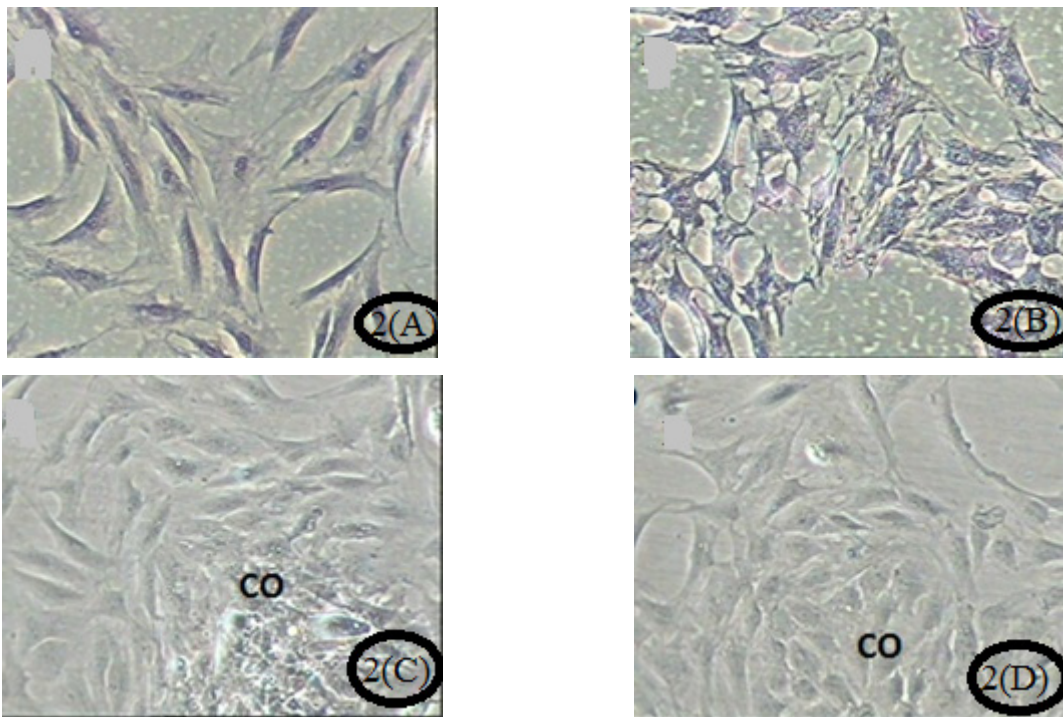


Fig. 2: (A&B): Two photomicrographs of AD-MSCs {1(A)} and BM-MSCs {1(B)} during the 1st passage, almost of the cells showed homogenous appearance with abundant cytoplasm and large nuclei. Each AD-MSC took a fibroblast-like shape while BM-MSCs tend to be polygonal in shape. 2(C&D): Phase contrasts of a rat AD-MSCs and BM-MSCs respectively showed large colonies (CO) with over growth of cells in layers in AD-MSCs 2(C) while BM-MSCs showed cell to cell contact growth inhibition 2(D). Gimsa Stain Scale Bar 100

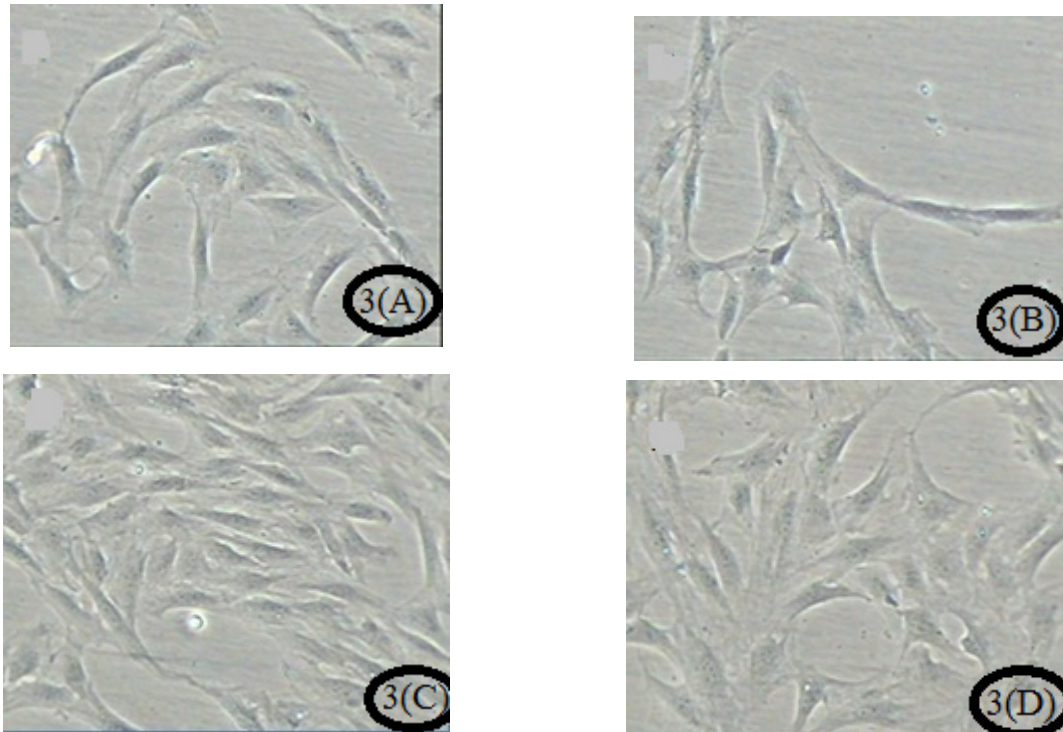
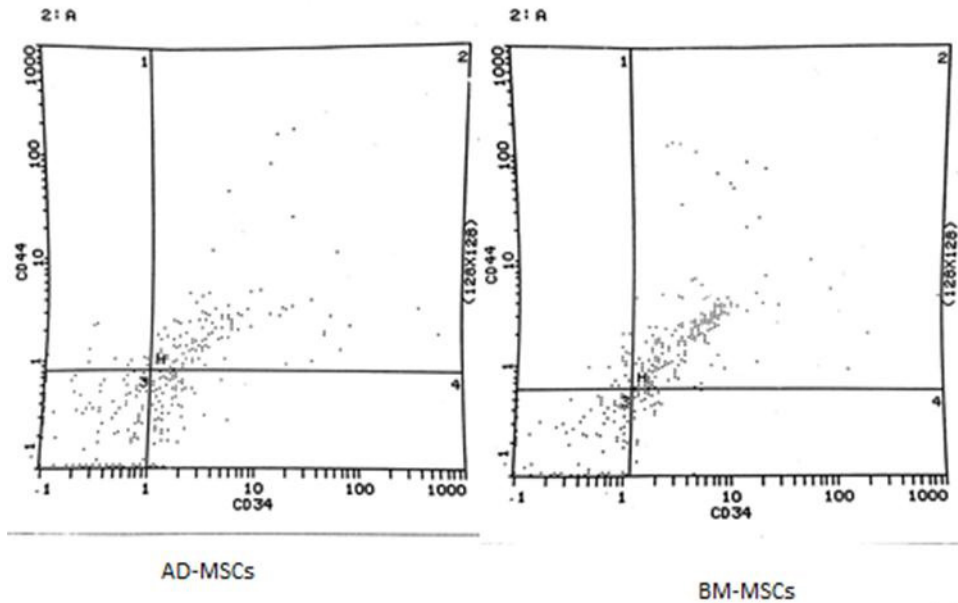
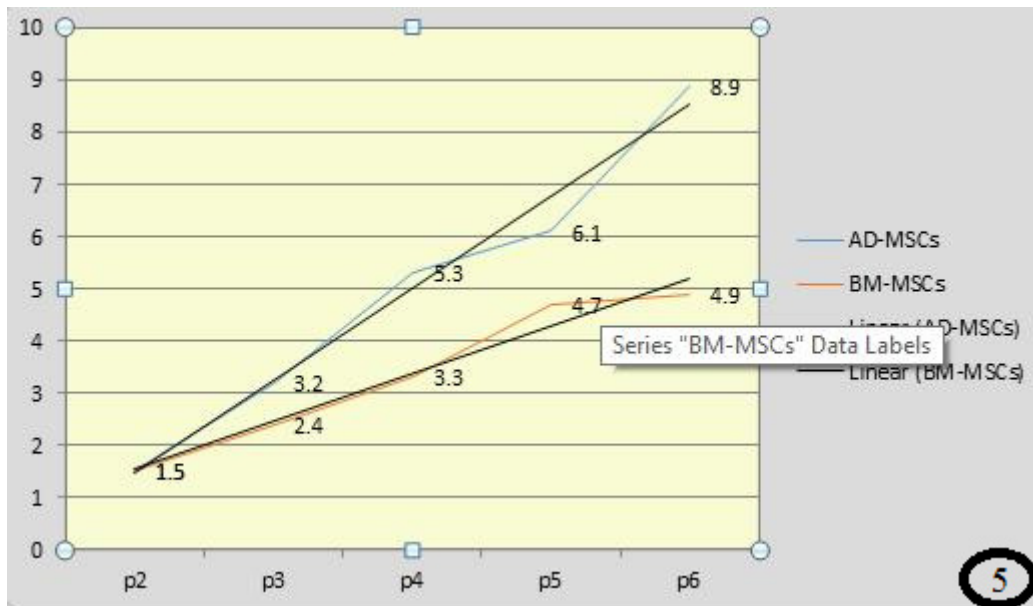


Fig. 3 (A, B, C&D): A phase contrast of AD-MSCs {3(A&C)} and BM-MSCs 3(B, D) during the 1st passage {3(A, B)} and the 3rd one {3(C&D)} showing the cells showed homogenous appearance with an abundant cytoplasm and large nuclei. Most of the cells took the fibroblast-like shape. Scale Bar 100



4

Fig. 4: A chart showing flow cytometry of a rat AD-MSCs and BM-MSCs during the 3rd passage. BM-MSCs exhibited specific MSC marker (CD44) at a higher level than that of Ad-MSCs (80% and 65% respectively) and hematopoietic cell markers (CD34) at a lower level than AD-MSCs (9% and 22%) respectively.



5

Fig. 5: A bar chart showing comparison of mean \pm SD of cell counts(X10⁵) in growth curves of rat bone marrow-derived mesenchymal stem cells (BM-MSCs) and adipose tissue-derived mesenchymal stem cells (AD-MSCs) between passages 2 and 6. The proliferation rate of Ad-MSCs and BM-MSCs increased gradually from passage 2 to passage 6 (trend lines). The number of AD-MSCs significantly exceeds that of BM-MSCs at almost all passages ($p < 0.05$).

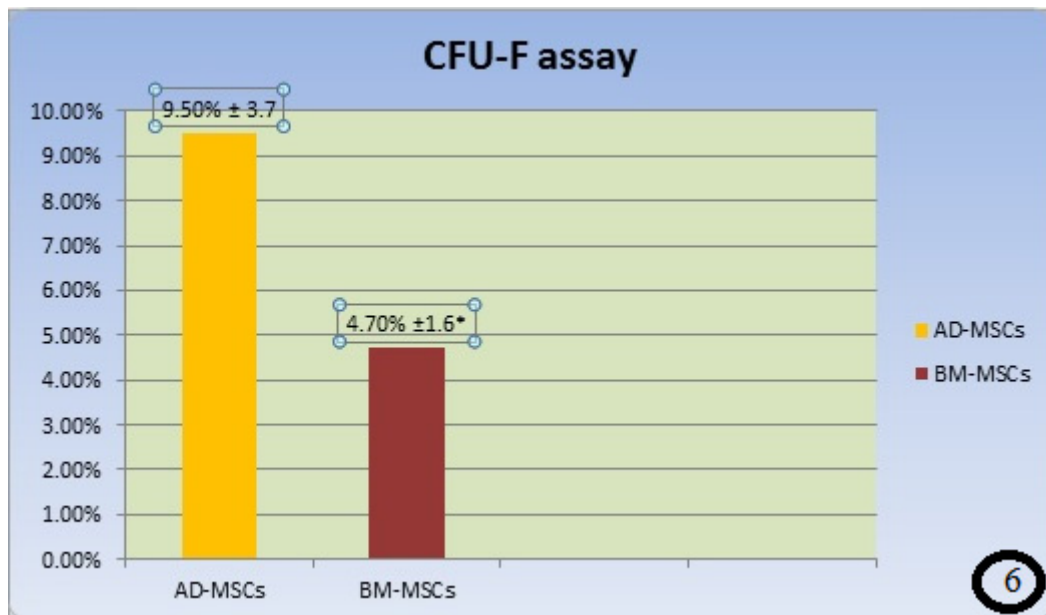


Fig. 6: A bar chart showing colony forming unit fibroblast assay (CFU-F assay) of rat AD-MSCs and BM-MSCs. AD-MSCs show a statistically significant increase of CFU-F assay in comparison to BM-MSCs during the 1st passage. *: P<0.05

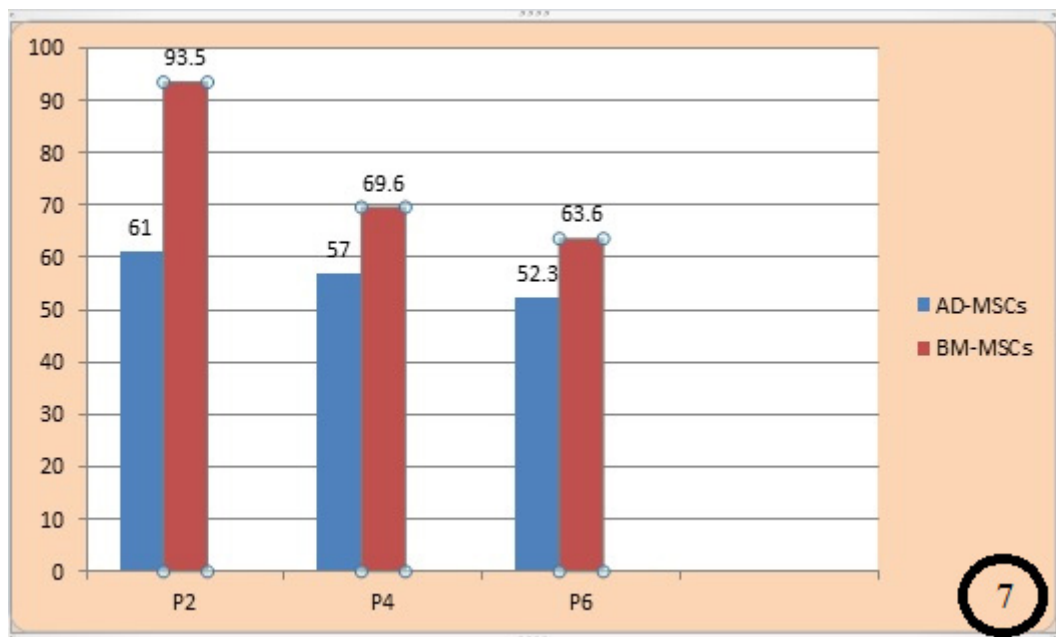


Fig. 7: A chart showing the population doubling time of rat AD-MSCs and BN-MSCs during the 2nd, 4th and 6th passages (P2, P4, and P6). There was a significant increase of AD-MSCs proliferative capacity in all these passages (P<0.05).

Table 1: Number of the rat AD-MSCs and BM-MSCs at the beginning and at the end of the 2nd, 4th and 6th passages and their population doubling time through these passages. The PDT decreased in both types of cells with the increase of the passage

AD-MSCs	Cell N. at the beginning of passaging	Cell N. at the end of passaging	PDT
Passage 2	20 000	53000	82.5 h*
Passage 4	20 000	57000	61.2h*
Passage 6	20 000	61000	52.3 h*
BM-MSCs	Cell N. at the beginning of passaging	Cell N. at the end of passaging	PDT
Passage 2	20 000	41000	93.5h
Passage 4	20 000	44000	69.6 h
Passage6	20 000	49000	63.6 h

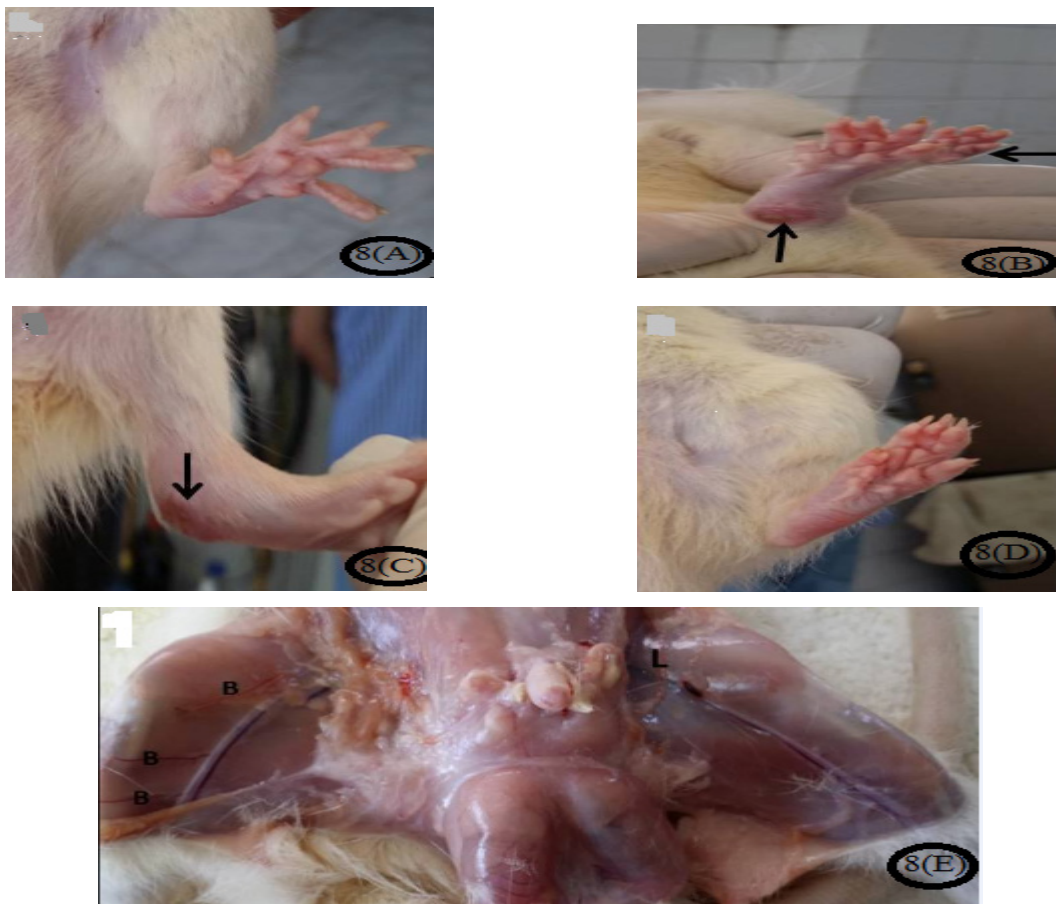


Fig. 8: (A, B, C, D&E): Photographs a rat model of the hind limb ischemia. 8(A): control group. 8(B): ischemic group, showing ulceration (↑) and toe necrosis (←) while BM-MSCS-treated group {8(C)} and AD-MSCS-treated group {8(D)}, showing an absence of these symptoms except for traces of healed ulcers in BM-MSCS-treated group (↓). 8(E): Showing site of ligation of the left femoral artery (L) with femoral vessels appeared faint while in the contralateral side the femoral vessels are obviously seen with a large number of muscular branches (B). X 1.5

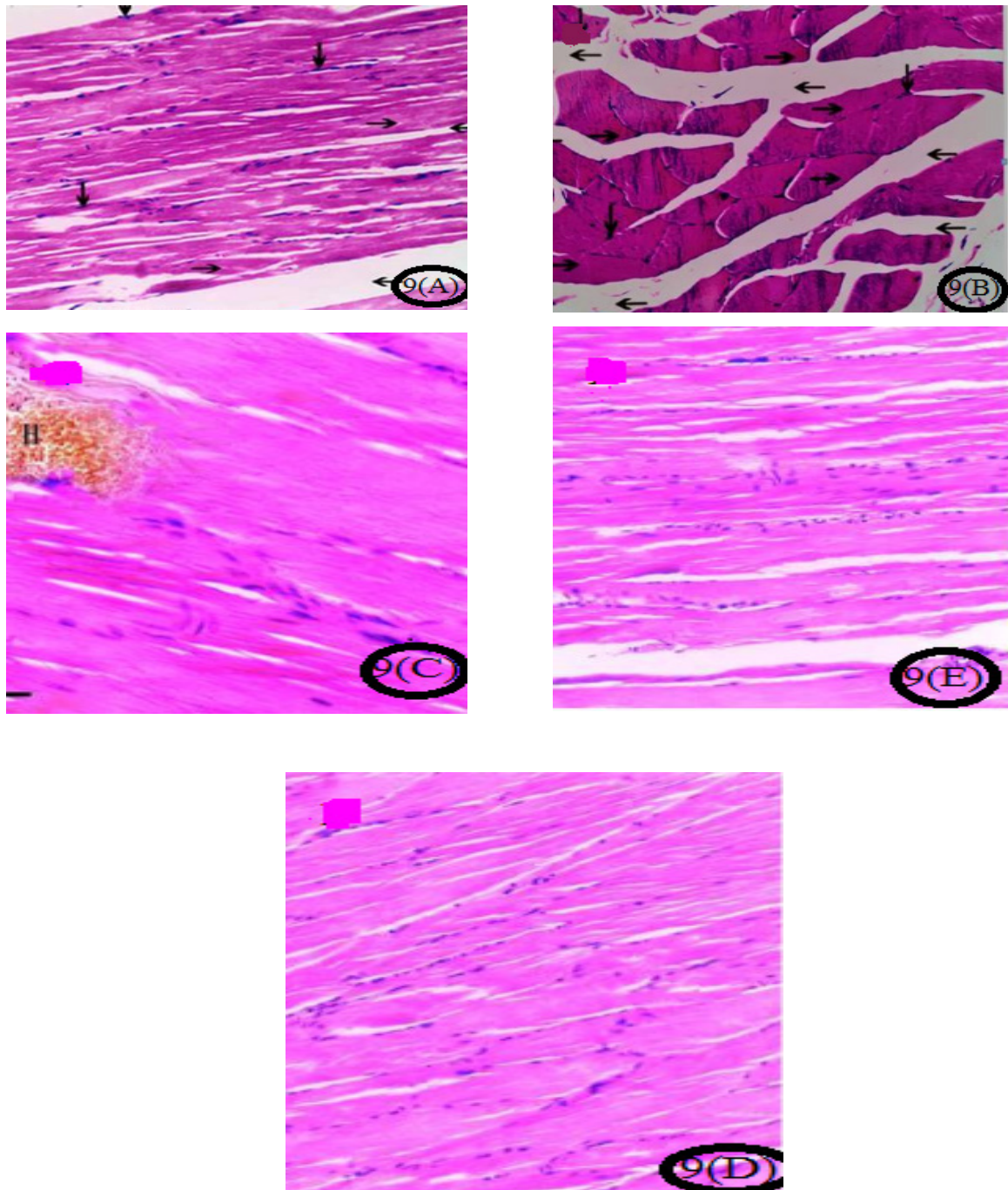


Fig. 9: (A, B, C, D&E): Photomicrographs of the semimembranosus sections of the rat model of hind limb ischemia. 9 (A&B): A longitudinal section and a transverse section from the control group respectively, showing the muscle fibers (→), with prominent peripheral vesicular nucleus (↓). The muscle fibers are separated from each other by a loose vascular connective tissue (←). 9(C): A longitudinal section from the ischemic group, showing disorganization of the muscle fibers and focal areas of hemorrhage (H). 9(D&E): Longitudinal sections from the ischemic groups treated with BM-MSCs and AD-MSCs respectively, showing organization of the muscle fibers. H&E X 200

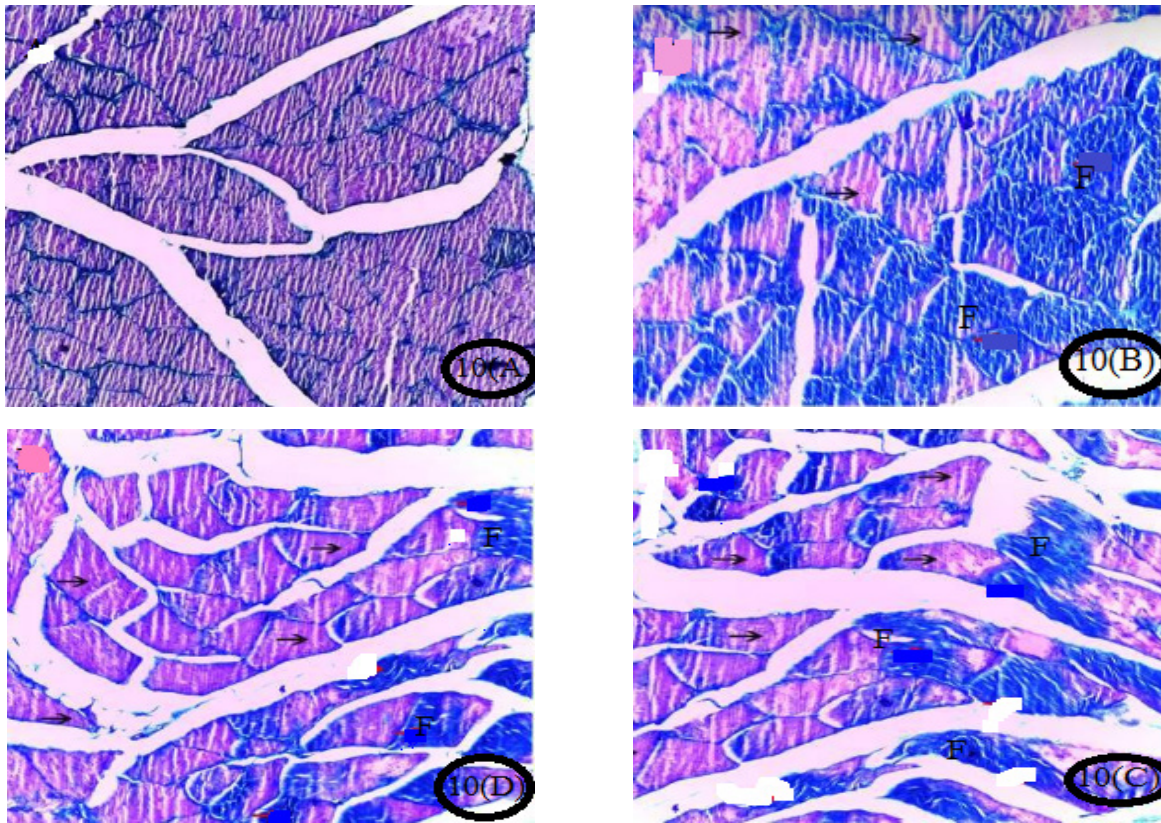


Fig. 10 (A, B, C&D): Photomicrographs of a transverse sections from the semimembranosus sections of rat model of the hind limb ischemia showing normal architecture of the muscle fibers of the control group {10(A)}, massive fibrosis (F), between the muscle fibers (→) in the ischemic group {10 (B)} in comparison to the control group {10(A)}, while the ischemic group treated with BM-MSCs and AD-MSCs {10(C&D, respectively)} showing moderate and mild areas of fibrosis (F), between the tissues of the muscle fibers (→). Masson Trichrome X 200

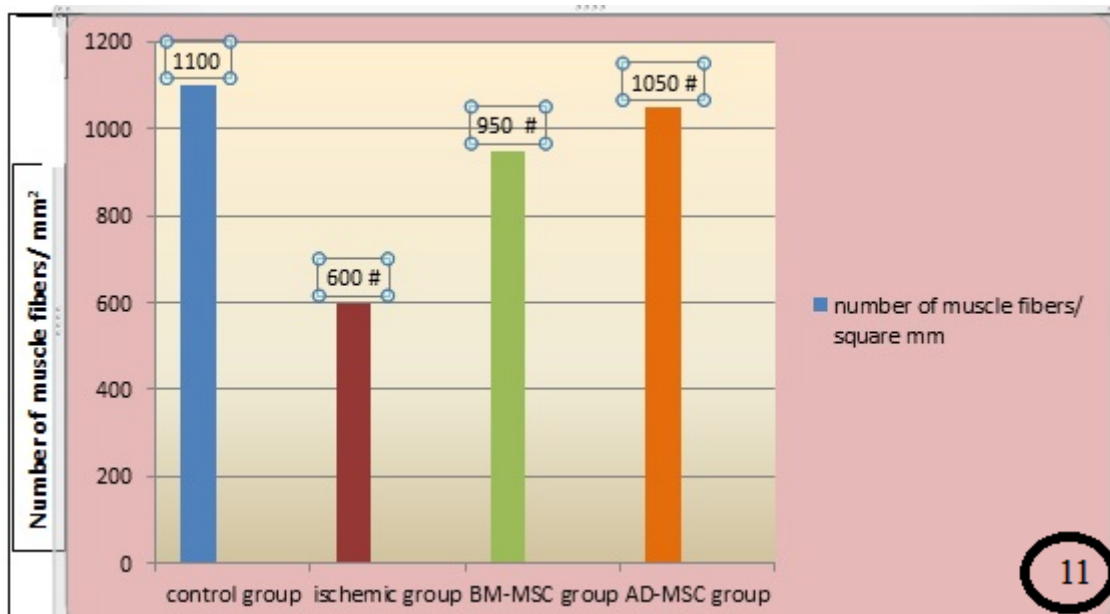


Fig. 11: Charts showing the number of muscle fibers/ mm² of rat semimembranosus sections of male rats after 6 weeks of femoral artery ligation. There was a significant muscular degeneration. *: P<0.01 #: P<0.05

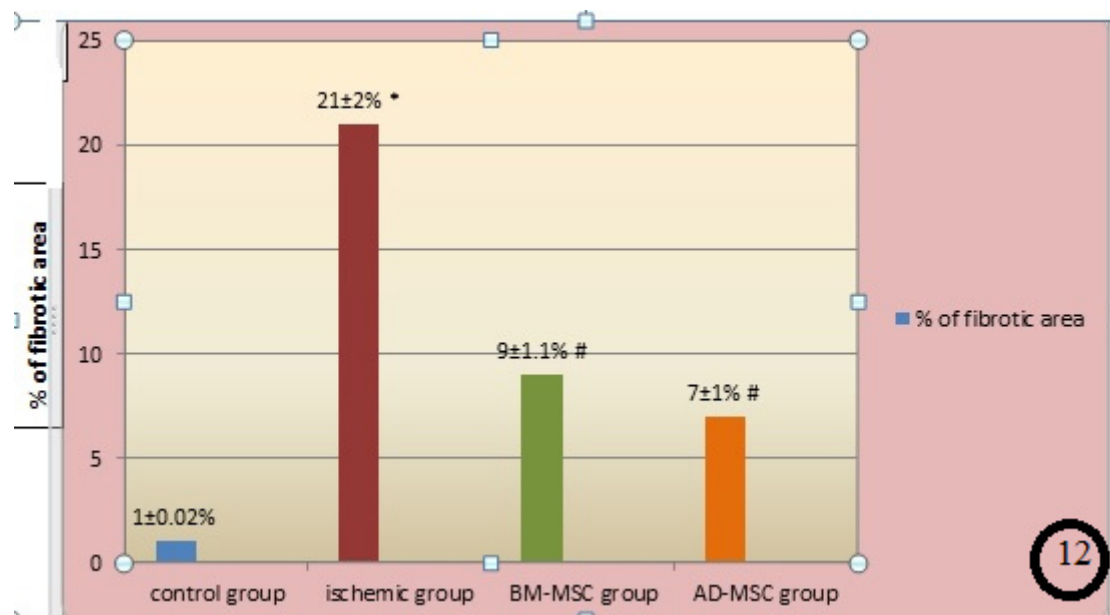


Fig. 12: Chart showing the percentage of fibrotic areas of rat semimembranosus sections of male rats after 6 weeks of femoral artery ligation. There was a significant an increase in the fibrotic area of the ischemic group in comparison to the control. Both BM-MSCs-treated group and AD-MSCs treated group showed a significant decrease in the percentage of the fibrotic area. *: P<0.01 #: P<0.05

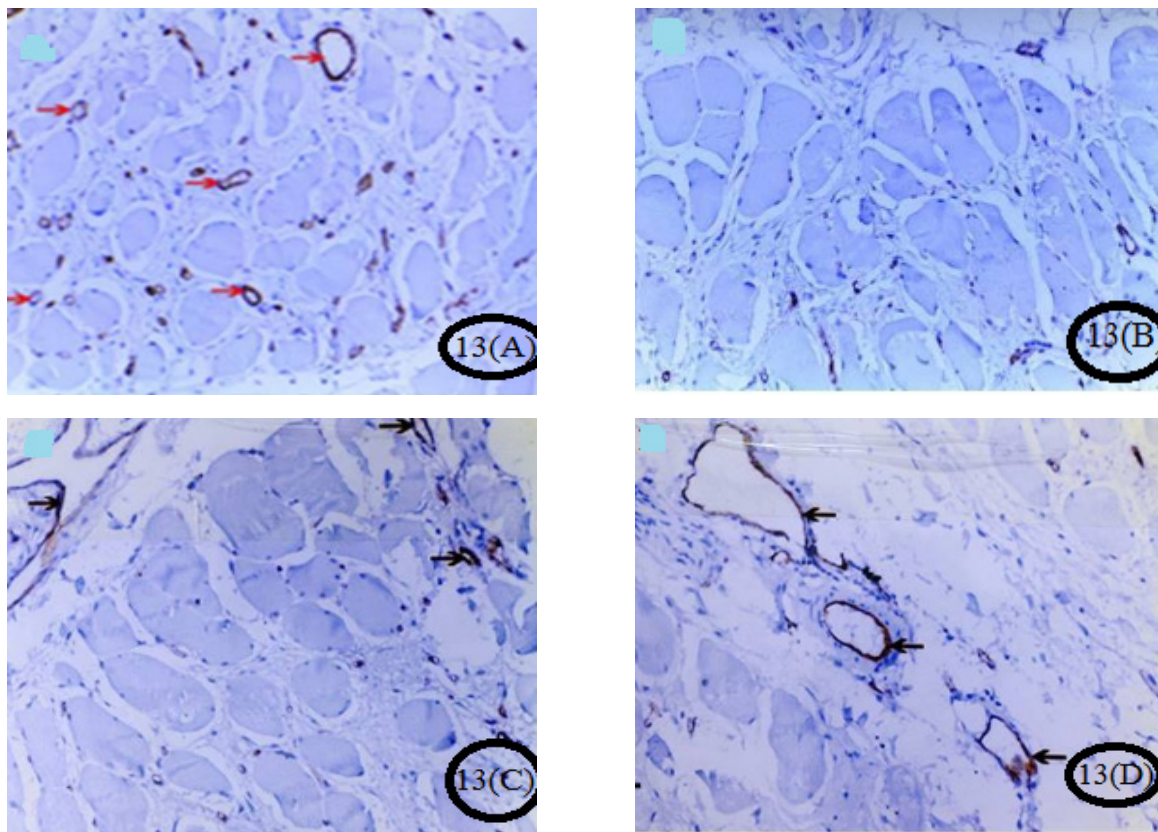


Fig. 13 (A, B, C&D): Photomicrographs of a transverse section from the semimembranosus muscle of the hind limb ischemia of a rat model immunohistochemically stained with anti CD31 antibody showing a week expression of this antibody in the control group {13(A)}, no expression in the ischemic group {13(B)} and a markedly high expression in both AD-MSCs and BM-MSCs treated groups {13(A&B), respectively} in the form of newly formed blood vessels with different shapes (arrow). CD31 X 200

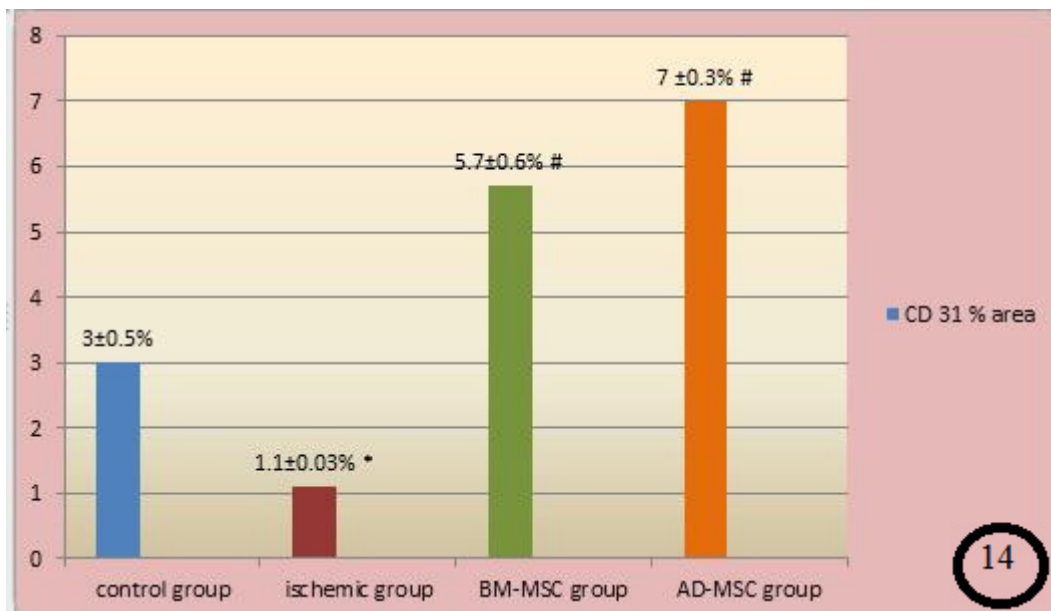


Fig. 14: A chart showing the capillary density (number of CD positively stained cells/ muscle fibers) of semimembranosus section of rat model of hind limb ischemia. There was a significant decrease of the capillary density in the ischemic group in comparison to the control group, a marked significant increase in it in both BM-MSCs-treated group and AD-MSCs treated group with a significant increase in the AD-MSCs treated group in comparison to the BM-MSCs-treated group. *: P<0.01 #: P<0.05

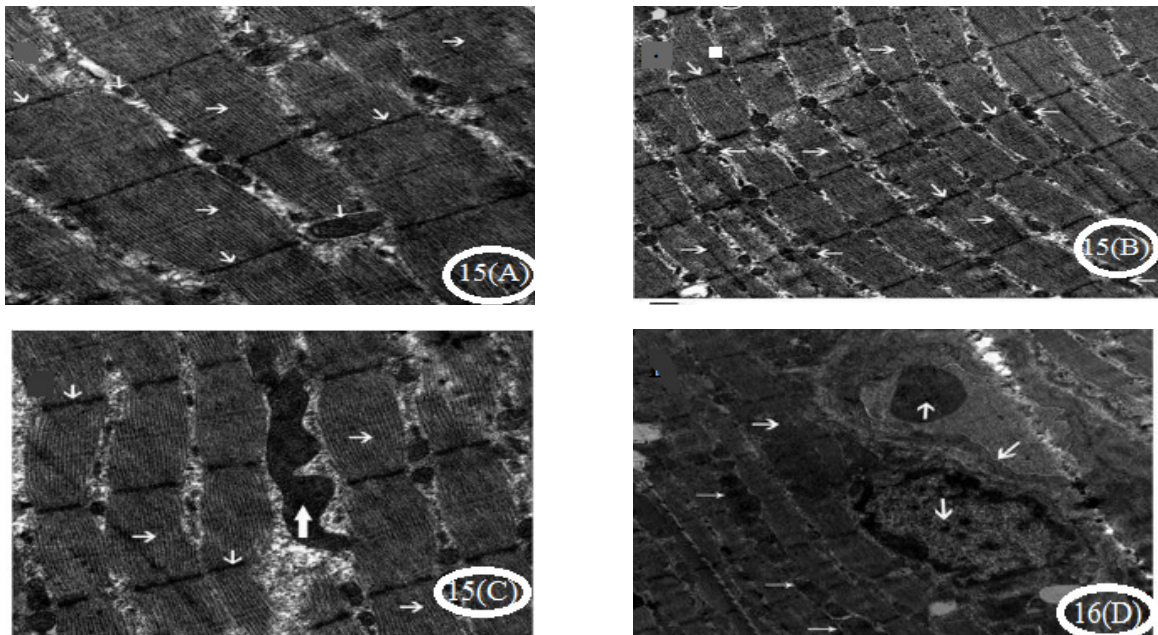


Fig. 15: (A, B, C&D): Electron micrographs of semimembranosus muscle of the control group. 15 (A & C): Showing the muscle fibers (→) with normal alignment of Z lines (↓). A blood vessel is seen (↑). 15(A): Longitudinally arranged rows of mitochondria (→) lie between the striated muscle fibers. 15(D): A peripherally situated nucleus is seen between the muscle fibers (↓) with a normal distribution of the chromatin and nucleoli inside the nucleus. A blood vessel is seen (↑) with its lining endothelium (↓). E. M. 15(A) X 25000 15(B) X 15000 15(C) X25000 15(D) X 12000

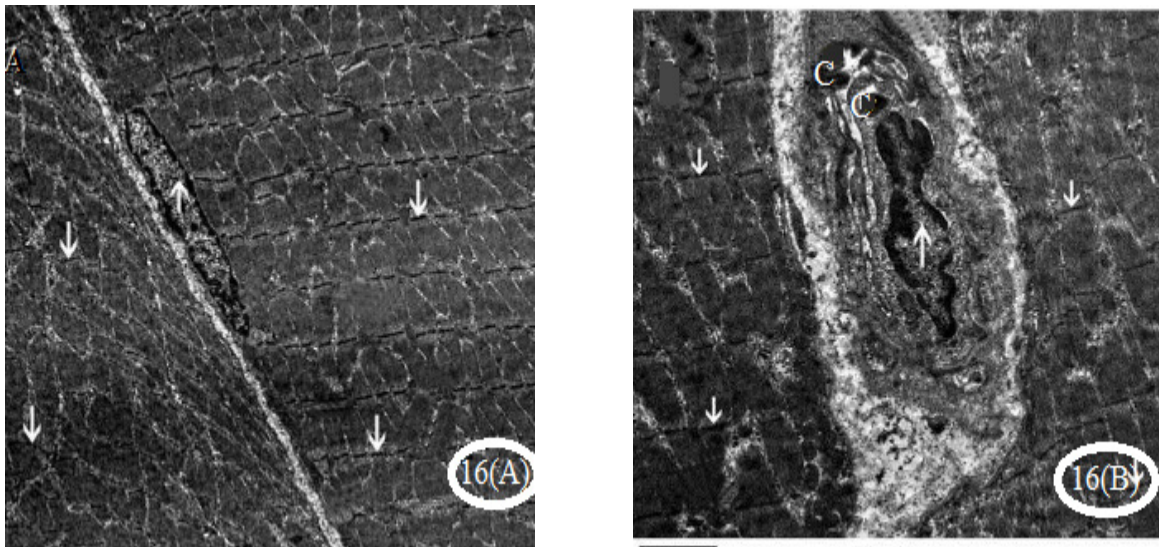


Fig. 16 (A&B): Electron micrographs of semimembranosus muscle of a rat model of the hind limb ischemia of the ischemic group showing distortion of the normal alignments of Z lines (↓) of the muscle fibers. 16 (B) A peripherally situated nucleus is seen between the muscle fibers (↑) with dispersion of the chromatin inside the nucleus (C).

E. M. 16(A) X 6000

16(B) X 10000

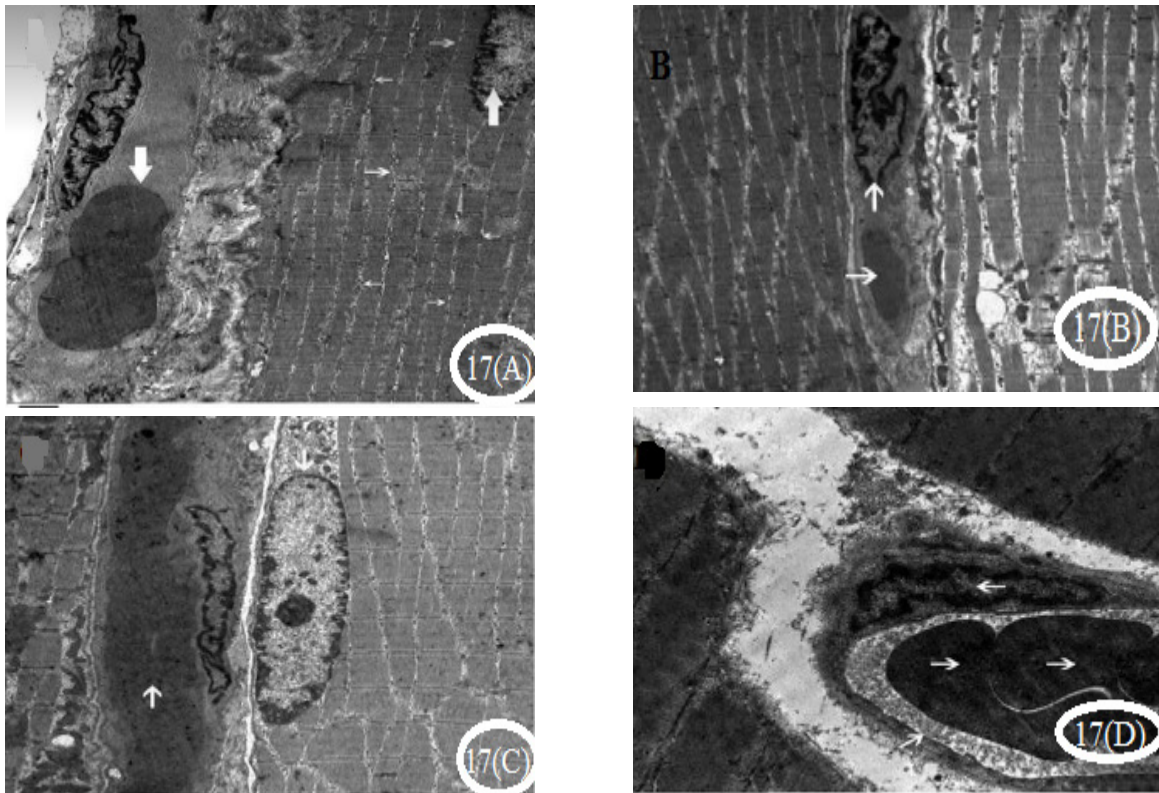


Fig. 17 (A, B, C&D): Electron micrographs of the semimembranosus muscle of a rat model of the hind limb ischemia, 17(A, B&C): AD-MSCS treated group showing restoration of the normal architecture of the skeletal muscle fibers (→) with peripherally situated nucleus between them (↑), 17(A) A large blood vessel (↓) is seen. 17(B): Two blood vessels are seen (→) with a nucleus in between (↑). 17(C): Showing large blood vessel (↑) with a peripheral nucleus (↓). 17(D): An electron micrograph of BM-MSCS of a rat of the treated group showing discoid and biconcave appearance of red blood cells inside it (→), with its lining endothelium and a peripheral nucleus (←).

E. M. 17(A) X 5000

17(B) X 5000

17(C) X 6000

17(D) X 12000

DISCUSSION:

Peripheral arterial disease (PAD) is one of the factors which lead to a decline of life quality and a high mortality and morbidity rates. Low efficiency of traditional therapy calls for alternative therapeutic strategies to improve the blood supply to save the ischemic limb.

In the current study we compare both BM-MSCs and AD-MSCs regarding their growth kinetics in vitro and their possible angiogenic properties in a rat model of hind limb ischemia. The results showed a significant relieve of hind limb ischemia accompanied by enhanced angiogenesis in vivo in both types of cells with great superiority of AD-MSCs that also showed a significant better growth kinetic in vitro in comparison to the BM-MSCs. this is a very inspiring to develop a new cell therapy based on these findings.

Being mesodermal in origin, both BM-MSCs and AD-MSCs have the plasticity to differentiate into originally mesoderm-derived cells, such as osteoblasts, chondrocytes, adipocytes and Vascular endothelial cells (Butler et al., 2012 and Yin et al., 2016). This makes them ideal candidates to promote angiogenesis and ultimately treat the ischemia through the tissue repair (Vishnubalaji et al., 2012).

The volume of bone marrow that could be harvested for any particular use was usually miniscule in comparison to the number of cells needed to regenerate the injured tissues besides the painful procedure and the significant morbidity while harvesting it (it has been estimated that MSCs represent only 0.001–0.01% of the total nucleated cells of bone marrow (Miao et al., 2006), while, the AD-MSCs are ubiquitous and easily obtained in great yield with little donor site morbidity and discomfort. This makes AD- MSCS an alternative promising cytotherapy (Kolaparthi et al., 2015). Our results revealed that the growth kinetics of AD-MSCs including the growth and proliferation rat and PDT were more significantly better than BM-MSCs. In other researches on rat, guinea pigs and human, it was proved that AD-MSCs seemed to have less percentage of senescent cells, more proliferation rate and higher expansion rate during the passaging than the BM-MSCs (Eslaminejad et al., 2008; Li et al., 2015 and Aliborzi et al., 2016). The higher proliferation capacity in AD-MSCs could be due to significant differences in

the gene expression patterns and higher expressed of cell division cycle associated 8 (CDCA8), and cyclin B2 (CCNB2) genes in AD-MSC than in BM-MSCs (Alipour et al., 2015). However, the species of the animal, the source of the samples, the cultivation conditions and various medium supplements may have an effect on PDT and proliferative rat of MSCs (Schipper et al., 2008).

In the current study, BM-MSCs and AD-MSCs showed morphological difference in primary culture. AD-MSCs appeared fibroblast like with longer cytoplasmic processes than that of BM-MSCs which tended to be polygonal in shape. While in late culture and subcultures both type of cells took the fibroblast-like appearance. These findings are consistent with the results of Nadri and Soleimani (2007) on the mice, Lotfy et al. (2014) on rats and that of Li et al. (2015) on the human MSCs. Besides, the AD-MSCs showed a significant higher colonogenic tendency in comparison to BM-MSCs. these results are concordant with those of Peng et al. (2008).

The isolated AD-MSCs in the current research had a typical immunophenotype similar to BM-MSCs including positive expression of CD 44 and the lack of hematopoietic cell surface marker CD34 but with a percentage dissimilarity. BM-MSCs express more CD44 and less CD34 than AD-MSCs. Li et al. (2015), stated in his research on human MSCs that there was a great similarity of expression of these markers on both types of cells. This difference may be caused by species difference or may be caused by the change of expression of these markers through a different passage; we characterized the cells through the 3rd passage while Li et al. (2015) characterized them during the 5th one. The similarity of immunophenotypes between the 2 types of cells confirmed the typical attributes of MSCs in the isolated, primary cultured and sub cultured AD-MSCs.

Our in vivo result in the rat model of the hind limb ischemia revealed that transplantation of BM-MSCs and AD-MSCs significantly improve the clinical picture, restore the normal architecture and the ultrastructure of the semimbranosus muscle, stimulate its regeneration and decrease the post ischemic fibrosis by enhancing angiogenesis and increasing blood flow and capillary density in the ischemic hind limb. These finding were significantly better

in the group that were subjected to AD-MSCs transplantation. It has been reported that MSCs from different tissues including adipose tissue (Baer & Geiger, 2012), bone marrow (Choi, et al., 2011), umbilical cord (Butler et al., 2012), skin (Vishnubalaji et al., 2012) and placenta (Xie et al., 2016) can differentiate into vascular endothelial cells, mount a successful repair response and restore the blood flow in the ischemic injuries.

New angiogenesis was evident in this study by the significant increase of CD 31 expression (a specific endothelial marker) in the MSCs treated groups in comparison to the control and the ischemic groups. Kong et al., 2013 stated that placental mesenchymal stem cells (PMSCs) acquire endothelial-like characteristics in vitro when cultured in endothelial induction media including expression of endothelial markers and formation of capillary-like structures when plated on a basement matrix gel. Also, PMSCs contribute in the new vessel formation in a mice model of the hind limb ischemia by an intravenous injection of FITC- labelled UEA-I to enhance the contrast of perfused vessels and assure its connection to the mouse circulatory system (Xie et al., 2016).

In addition to the new angiogenesis which is a pre request to save an ischemic limb, the anti-apoptotic, anti-inflammatory and immunomodulatory properties of MSCs may contribute to improve the prognosis of limb ischemia, stimulate muscle regeneration and prevent limb necrosis and auto amputation. Also the paracrine factors secreted by MSCs might contribute to the angiogenesis in multiple animal models (Xiao-Yun et al., 2011 and Kong et al., 2013). BM-MSCs were proved to produce VEGF (Shen et al. 2016) and IL-8 (Wang et al., 2015). AD-MSCs also secrete VEGF (Lauvrud et al., 2016) all of which are paracrine angiogenic factors which promotes angiogenesis.

The main limitation of using MSCs as a cytotherapy in the limb ischeamia is the maintenance of these cells viable in a sufficient number and for a sufficient time allowing for new angiogenesis after transplantation (Fakoya, 2017) which depends on many factors including the route of cell administration, their number, time and frequency of administration. Clinical trials using intramuscular and intravascular injections, or a combination of both, with variable cellular number have produced a favorable

results, however, intramuscular injection into the semimembranosus muscle has been the preferred application in most trials to avoid cell trapping in the pulmonary circulations when transplanted intravenously so we used the same protocol and similar results were achieved (Gyongyosi et al., 2009, Xie et al, 2015). Intramuscular delivery results in a transient cell depot directly within the ischemic tissue site to allow both local paracrine activity as well as incorporation of cells into the newly formed vessels (Cooke and Losordo, 2015). However, dose-dependent ulcer healing improvement and rest pain reduction in those treated with an intra-arterial administered of BM-MNC compared with the placebo group (Walter et al., 2011) was reported.

CONCLUSION

This study successfully isolated the rat BM-MSCs and AD-MSCs, comparing their growth kinetics in vitro and their role as cytotherapy in a rat model of hind limb ischemia. AD-MSCs showed a significant higher growth and proliferation rate than BM-MSCs. Both types of cells were proved to relieve hind limb ischemia effectively and efficiently by promotion of angiogenesis marked by expression of CD31 endothelial marker and restoration of the structure and ultrastructure of the semimembranosus muscle. Better improvement was observed with AD-MSCs transplantation; these results make them ideal candidates to provide a promising therapeutics for relieving the limb ischemia.

REFERENCES

- Alipour, F., Parham, A., Mehrjerdi H.K. and Dehghani H. 2015. Equine adipose-derived mesenchymal stem cells: phenotype and growth characteristics, gene expression profile and differentiation potentials. *Cell J* 16:456-46.
- Baer, P.,C and Geiger, H. 2012. Adipose-derived mesenchymal stromal/ stem cells: tissue localization, characterization, and heterogeneity. *Stem Cells Int*; vol. 330, no. 1, pp. 142–150.
- Butler, J.M.; Gars, E.J.; James, D.J. et al.2012. Development of a vascular niche platform for expansion of repopulating human cord blood stem and progenitor cells. *Blood.*; 120: 1344–1347.

- Choi, Y. H.; Kurtz, A. and Stamm C. 2011.** Mesenchymal stem cells for cardiac cell therapy. *Hum Gene Ther.* 22: 3–17.
- Das, B., Abdullah, S., Dhillon, A., Vijanari, C., and Gupta, P. 2013.** "Intra-arterial allogeneic mesenchymal stem cells for critical limb ischemia are safe and efficacious: report of a phase I study". *World Journal of Surgery*, 37(4):,915–922.
- Eslaminejad, M. B.; Mardpour, S. and Ebrahimi, M. 2008.** Growth kinetics and in vitro aging of mesenchymal stem cells isolated from rat adipose versus bone marrow tissues. *Iran J Vet Surg.* 3:9-20.
- Fakoya, J. 2017.** New Delivery Systems of Stem Cells for vascular Regeneration in ischemia. *frontiers in cardiovascular medicine.* *Front. Cardiovasc. Med.* 4:7.
- Gresele, P.; Bufti, C. and Fierro, T. 2011.** Critical limb ischemia. *Intern Emerg Med* 6:129-134.
- Gyongyosi, M.; Lang, I.; Dettke, M. et al. 2009.** Combined delivery approach of bone marrow mononuclear stem cells early and late after myocardial infarction: the MYSTAR prospective, randomized study. *Nat Clin Pract Cardiovasc Med.* 6(1):70–81.
- Hart, J., Tsui, A., Khanna, D., and Baker, D. 2013.** "Stem cells of the lower limb: their role and potential in management of critical limb ischemia." *Experimental Biology and Medicine*, 238(10) 1118–1126.
- Huang, N. F., Niiyama, H., De, A., Cooke, J. P. 2008.** Transplantation and non-invasive tracking of embryonic stem cell-derived endothelial cells for treatment of hindlimb ischemia. *J Vis Exp J Vis Exp*; (23): 1035.
- Jo, C.H.; Kim, O.S.; Park, E.Y. et al. 2008.** Fetal mesenchymal stem cells derived from human umbilical cord sustain primitive characteristics during extensive expansion. *Cell Tissue Res.*, 334, 423–433.
- Kakudo, N.; Morimoto, N.; Ogawa, T. and Kusumoto, K. 2014.** Potential of adipose-derived stem cells for regeneration medicine: clinical application and usefulness of fat grafting. *J Stem Cell Res & Ther.* 4(5):1000204.
- Katare, R., Riu, F., Rowlinson, J., et al. 2013.** Perivascular delivery of encapsulated mesenchymal stem cells improves postischemic angiogenesis via paracrine activation of VEGF-A. *Arteriosclerosis, Thrombosis, and Vascular Biology*, 33(8), 1872–1880.
- Kolaparthi, L. K.; Sanivarapu, S.; Moogla, S. and Kutcham, R. S. 2015.** Adipose tissue – Adequate, accessible regenerative material. *Int J Stem Cells.* 8:121-127.
- Kong, P.; Xie, X.; Li, F. et al. 2013.** Placenta mesenchymal stem cell accelerates wound healing by enhancing angiogenesis in diabetic Goto-Kakizaki (GK) rats. *Biochem Biophys Res Commun.* 438: 410–419.
- Kretlow, J.D.; Jin, Y.Q.; Liu, W. et al. 2008.** Donor age and cell passage affects differentiation potential of murine bone marrow-derived stem cells. *BMC Cell Biol.* 9:60, doi:10.1186/1471-2121-9-60.
- Lauvrud, A.T., Kelk, P., Wiberg, M., and Kingham, P.J. 2016.** Characterization of human adipose tissue-derived stem cells with enhanced angiogenic and adipogenic properties. *J Tissue Eng Regen Med.* 11(9):2490-2502.
- Li, C.; Wu, X.; Tong, J. et al. 2015.** Comparative analysis of human mesenchymal stem cells from bone marrow and adipose tissue under xeno-free conditions for cell therapy. *Stem Cell Research & Therapy* 13;6:55.
- Lotfy, A.; Salama, M.; Zahran, F.; Jones, E.; Badawy, A. and Sobh, M. 2014.** Characterization of Mesenchymal Stem Cells Derived from Rat Bone Marrow and Adipose Tissue: A Comparative Study. *International Journal of Stem Cells* 7(2): 135-142.
- Mees, B.; Recalde, A. and Loinard, C. 2011.** Endothelial nitric oxide synthase overexpression restores the efficiency of bone marrow mononuclear cell-based therapy. *Am J Pathol*; 178:55–60
- Miao, Z., Jin, J., Chen, L. et al. 2006.** Isolation of mesenchymal stem cells from human placenta comparison with human bone marrow mesenchymal stem cells. *Cell Biol Int.* 30: 681–687.
- Nadri, S. and Soleimani, M. 2007.** Isolation murine mesenchymal stem cells by positive selection. *In Vitro Cell Dev. Biol. Anim.* 43:276-282.

- Niyaz, M.; Gurpinar, O. A.; Gunaydin, S. and Onur, M.A. 2012.** Isolation, culturing and characterization of rat adipose tissue-derived mesenchymal stem cells: a simple technique. *Turk J Biol* 36, 658-664.
- Peng, L.; Jia, Z.; Yin, X. et al. 2008.** Comparative analysis of mesenchymal stem cells from bone marrow, cartilage, and adipose tissue. *Stem Cells Dev.* 17, 761-773. Schipper, B.M., Marra, K.G., Zhang, W., Donnenberg, A.D. and Rubin, J.P. 2008. Regional anatomic and age effects on cell function of human adipose-derived stem cells. *Ann Plast Surg* 60:538-544.
- Shen, C.C., Chen, B., Gu, J.T. et al. 2016.** The angiogenic related functions of bone marrow mesenchymal stem cells are promoted by CBDL rat serum via the Akt/Nrf2 pathway. *Exp Cell Res.* 15;344(1):86-94.
- Shimamura, M., Nakagami, H., Koriyama, H., Morishita, R. 2013.** Gene therapy and cell-based therapies for therapeutic angiogenesis in peripheral artery disease. *BioMed Research International*, 186215.
- Terai, S.; Sakaida, I.; Yamamoto, N. et al. 2003.** An in vivo model for monitoring trans-differentiation of bone marrow cells. *J Biochem*; 134:551-558.
- Vishnubalaji ,R., Manikandan, M., Al-Nbaheen, M. et al. 2012.** In vitro differentiation of human skin-derived multipotent stromal cells into putative endothelial-like cells. *BMC Dev Biol.* 27: 12-17.
- Walter , D. H.; Krankenberg, H.; Balzer, J. O. et al. 2011.** Intraarterial administration of bone marrow mononuclear cells in patients with critical limb ischemia: a randomized-start, placebo-controlled pilot trial (PROVASA). *Circ Cardiovasc Interv.* 1;4(1):26-37.
- Wang ,S., Qu, X., and Zhao, R. 2012.** Clinical applications of mesenchymal stem cells. *J Hematol Oncol.* 30;5:19.
- Wang, Q.; Yang, Q.; Wang, Z. 2015.** Comparative analysis of human mesenchymal stem cells from fetal-bone marrow, adipose tissue, and Warton's jelly as sources of cell immunomodulatory therapy. *Hum. Vaccin Immunother.*12(1):85-96.
- Xiao-Yun ,X., Zhao-Hui ,M., Ke, C., et al. 2011.** Glucagon-like peptide-1 improves proliferation and differentiation of endothelial progenitor cells via upregulating VEGF generation. *Med Sci Monit.* 17: 35-41
- Xie, T. and Spradling, A. 2016.** Dpp ? Is Essential for the Maintenance and Division of Germline Stem Cells in the Ovary. *Cell.* 94 (2): 251-260.
- Yin, T., He, S., Su, C., et al. 2015.** Genetically modified human placenta-derived mesenchymal stem cells with FGF-2 and PDGF-BB enhance neovascularization in a model of hindlimb ischemia. *Molecular Medicine Reports*, 12(4) 5093-5099.
- Yoshimatsu, G.; Sakata, N.; Tsuchiya1, E. et al. 2015.** The Co-Transplantation of Bone Marrow Derived Mesenchymal Stem Cells Reduced Inflammation in Intra-muscular Islet Transplantation. *Cell Tissue Res.* 327:449-462.

الخلايا الجذعية المستمدة من الأنسجة الدهنية مقابل الخلايا الجذعية المستمدة من نخاع العظام كعلاج مجدد للأوعية الدموية بعد الإصابة بالاسكيمية الطرفية في الجرذان البيضاء البالغين الذكور

محمد البدرى محمد¹، منى حسن محمد على²، مها محمد أبوجازية³، رانيا عبدالعظيم أبو جلهوم⁴ و أميرة السيد فرج⁵

قسم التشريح الأدمى وعلم الأجنة، كلية الطب، جامعة أسيوط¹

قسم التشريح الأدمى وعلم الأجنة، كلية الطب، جامعة قناة السويس²

قسم الهستولوجى ، كلية الطب، جامعة كفر الشيخ³

قسم التشريح الأدمى وعلم الأجنة، كلية الطب، جامعة كفر الشيخ⁴

ملخص البحث

خلفية: تعد امراض الشرايين الطرفية من الامراض المزمنة الاكثر انتشارا في العالم. يؤدي هذا المرض الي ضيق الشرايين الطرفية بدوره يؤدي الي نقص تدفق الدم والاكسجين والمواد الغذائية للساقين والقدمين. وتقتصر العلاجات الطبية لتخفيف الأعراض ، ولكن النتائج طويلة الأجل غالباً ما تكون مخيبة للآمال لذلك هناك حاجة إلى تطوير علاجات جديدة ، لذلك اتجه العلماء للعلاج عن طريق زرع الخلايا الجذعية. **الهدف من الدراسة:** فصل الخلايا الجذعية المشيمية المتوسطة من كل من نخاع العظام من الفئران وكذلك من الأنسجة الدهنية من الفئران المقارنة بين فصل وبين خصائص كل من الخلايا الجذعية المشيمية المتوسطة المشتقة من كل من نخاع العظام والأنسجة الدهنية للفئران ودورها في النمو التجديدي للأوعية الدموية بعد حدوث تنكز في الفأر الأبيض الذكر.

مواد وطرق البحث: تم فصل الخلايا من عدد 10 فئران بيضاء بالغة تم زراعتها في وسط مناسب مع السماح بتمدها وتزايدها في العدد ثم مقارنة معدل نموها وحساب الوقت اللازم لتضاعف عددها. ثم زرعها بعد حدوث تنكز حاد عن طريق ربط الشريان الفخذي الأيسر. خصائص الخلايا الجذعية المشيمية المتوسطة التي تم فصلها من نخاع العظام ومن النسيج الدهني تم ايضاحها بالشكل الظاهري و باستخدام الصبغة الهستولوجية. كما تم توصيف الخلايا الجذعية المشيمية المنفصلة عن طريق التدفق الخلوي لكل من سي دي 34 و سي دي 44 كما تم تحديد المنحني النموي لكل من النوعين من الخلايا لتحديد معدل النمو الخلوي خلال التمرير الثاني والرابع والسادس للخلايا ويتم حسابها مجهرياً باستخدام الهيموسيتوميتر لانتاج منحني نمو الخلايا. وقد تم تشكيل المستعمرات التي تنتجها الخلايا الليفية وتم صبغتها بصبغة جيمسا للمقارنة بين الخلايا الجذعية من نخاع العظام ومن الأنسجة الدهنية وقد تم أخذ عينات من نسيج العضلات من كل المجموعات وصبغتها بصبغة الهيماتوكسيلين والايوسين وصبغه الماسون تريبكروم وفحصها بالميكروسكوب الضوئي لمعرفة شكل الخلايا ومعرفة التغيرات في تجدها بعد زرع كلا من الخلايا الجذعية المشتقة من كل من نخاع العظام والخلايا الدهنية كما تم أخذ عينات أخرى من العضلات وتم فحصها بالميكروسكوب الإلكتروني لمعرفة التركيب الدقيق لخلايا النمو التجديدي. كما تم قياس مستقبلات عامل منشط الأوعية الدموية بنسج العضلات باستخدام المضاد المناعي له.

نتائج البحث : معدل نمو الخلايا الجذعية الشحمية أكبر من مثيله في الخلايا الجزعية المنفصلة من نخاع العظام حيث ان الوقت اللازم لتضاعف عددها اقل من الخلايا الجذعية المشتقة من نخاع العظام. وقد وجد انه بالرغم من وجود تشابهات كثيرة بين النوعين من الخلايا من حيث الشكل المورفولوجي بعد الفصل من نخاع العظام ومن النسيج الدهني الا ان هناك بعض الاختلافات التي يمكن أن تساهم في اختيار نوع الخلايا لاستخدامها في الاغراض العلاجية المختلفة. كما وجد تحسن في تجدد النسيج العضلي بعد الحقن بالخلايا الجذعية المشتقة من النسيج الدهني بمعدل افضل من تلك التي وجدت في المجموعه التي تم فيها الحقن بالخلايا الجذعية المشتقة من نخاع العظام وذلك عن طريق الاوعية الدموية الجديدة التي كونتها الخلايا الجذعية.

الاستنتاج: في هذه الدراسة تم فصل الخلايا الجذعية المشيمية المتوسطة من كل من نخاع العظام من الفئران وكذلك من الأنسجة الدهنية من الفئران والمقارنة بين فصل وبين خصائص كل من الخلايا الجذعية المشيمية المتوسطة المشتقة من كل من نخاع العظام والأنسجة الدهنية للفئران ودورها في النمو التجديدي للأوعية الدموية بعد حدوث تنكز حاد في الفأر الأبيض الذكر. وقد وجد ان معدل نمو الخلايا الجذعية الشحمية أكبر من مثيله في الخلايا الجزعية المنفصلة من نخاع العظام. كما لوحظ ان كلا من الخلايا الجذعية المشتقة من كل من نخاع العظام والمشتقة من النسيج الدهني لها دور في النمو التجديدي للنسيج العضلي بعد الحقن بها وذلك عن طريق الاوعية الدموية الجديدة التي كونتها الخلايا الجذعية وتم قياسها بواسطة عامل منشط الأوعية الدموية كإتمام تجدد النسيج العضلي بعد التنكز وفحصه بكل من الميكروسكوب الضوئي والإلكتروني.